ORIGINAL PAPER

Synthesis and proton incorporation in BaCe$_{0.9-x}$Zr$_x$Y$_{0.1}$O$_{3-\delta}$

S. Ricote · G. Caboche · O. Heintz

Abstract BaCe$_{0.9-x}$Zr$_x$Y$_{0.1}$O$_{3-\delta}$ powders were synthesized by a solid-state method at 1,400 °C. Two compositions were studied ($x = 0.3$ and $x = 0.7$). Pellets were prepared and conventionally sintered in air at 1,700 °C. Then, the samples were heated at 600 °C for 3 h in different reducing atmospheres: dry hydrogen, wet hydrogen and wet deuterium. After each treatment, the proton diffusion depth profile was obtained using Secondary Ion Mass Spectroscopy (SIMS). Protons were not incorporated in the material when the gas was not wet, and the isotope effect suggests that protons present in the pellet come from water and not from hydrogen.

Keywords Protonic conductor · Cerates · Zirconate · Proton diffusion depth profile

1 Introduction

One way to offset the too high operating temperature of SOFCs (700–1,000 °C) is the use of a proton conducting electrolyte instead of an oxide conducting electrolyte [1–3]. Rare-earth substituted ABO$_3$ (A = alkaline earth, B = Ce, Zr, Ti) perovskites are studied for this application because of their high proton conductivity at 600 °C and their stability in reducing atmosphere [4]. Barium cerates exhibit high protonic conductivity but they react with carbon dioxide to form carbonates [5–8]. Barium zirconates are chemically and

S. Ricote (✉) · G. Caboche · O. Heintz
Institut Carnot de Bourgogne UMR 5209 CNRS ESIREM,
Université de Bourgogne, 9 Avenue Savary, P. O. Box 47870,
21078 Dijon Cedex, France
e-mail: sandrine.ricote@risoe.dk

mechanically stable but their protonic conductivity is quite low [9–12]. An oxide with both cerium and zirconium shows a satisfactory protonic conductivity and sufficient stability, and can be used as electrolyte in a Protonic Ceramic Fuel Cell (PCFC) [8, 13].

This study deals with BaCe$_{0.9-x}$Zr$_x$Y$_{0.1}$O$_{3-\delta}$ powders ($x = 0.3$ (powder referred to BCZY63) and $x = 0.7$ (BCZY27)). The minimal value chosen for x was 0.3 because a compound with more than 60% of cerium atoms is not stable after CO$_2$ treatment [13] and the lattice is orthorhombic. Kreuer pointed out a decrease in protonic defect mobility when the perovskite structures deviated from cubic [9]. A trivalent dopant such as yttrium is added to create oxygen vacancies by charge compensation [1, 2, 4, 14].
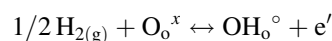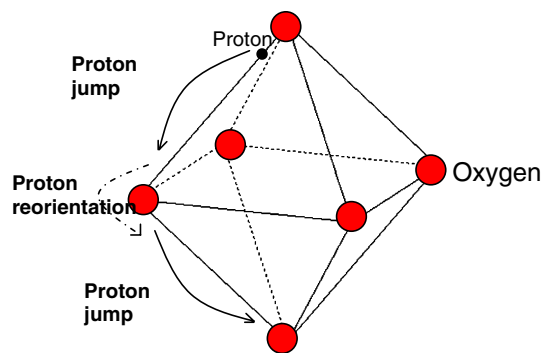
Protons can be incorporated into the material by the absorption and dissolution of water molecules in the oxygen vacancies [15–17]:

Reaction 1:

$$H_2O_{(g)} + V_o^{\circ\circ} + O_o^x \leftrightarrow 2\,OH_o^{\circ}$$
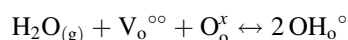
Others [14] mention the formation of protonic defects using only hydrogen:

Reaction 2:

$$1/2\,H_{2(g)} + O_o^x \leftrightarrow OH_o^{\circ} + e'$$

Proton transfer occurs with the Grotthuss diffusion mechanism (Fig. 1) for which protons move between stationary host anions [3, 14, 17–19]. This is a two-step mechanism which involves both a proton-transfer and a reorientation step [3, 20].

The aim of the present work is to verify, for two selected promising barium cerate compounds, the incorporation of protonic defects when heated in wet reducing atmosphere, and to study the proton diffusion.

Fig. 1 Grotthuss or free-proton mechanism

2 Experimental

Polycrystalline $BaCe_{0.9-x}Zr_xY_{0.1}O_{3-\delta}$ powders ($x = 0.3$ and 0.7) were produced by a solid state reaction. $BaCO_3$ (Aldrich, 99+%), CeO_2 (Aldrich, 99.9%, <5 µm), Y_2O_3 (Sigma-Aldrich, 99.99%), YSZ (Aldrich, submicron powder; 99.5%, 5.3 wt.% of yttria) commercial reactants were mixed together in a ball mill for 20 h and then calcined at 1,400 °C for 24 h in air.

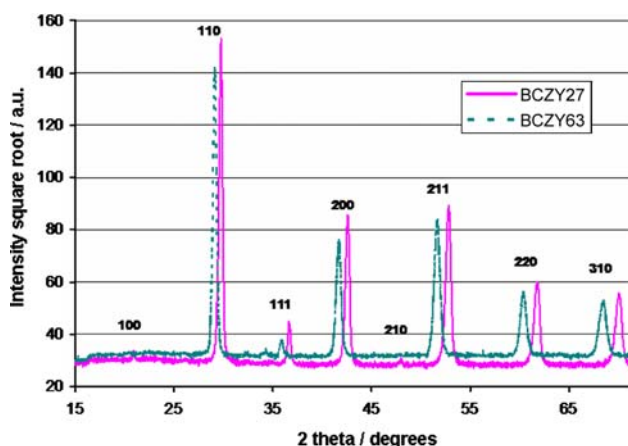**Fig. 2** XRD patterns for BCZY27 and BCZY63 powders, synthesized at 1,400 °C

Table 1 BCZY powders lattice parameters and density

Powder	Lattice parameter/Å	Density/g cm^{-3}
BCZY27	4.242	6.207
BCZY63	4.331	6.232

Crystallographic phases, lattice parameters and theoretical density were determined with a standard X-ray diffractometer INEL CPS 120 using Cu $_{K\alpha1}$ radiation.

SEM (Scanning Electron Microscope, Stereoscan 120 Cambridge) pictures were recorded to assess the particle morphology, with a 15 keV accelerating voltage.

Binding materials (Dolapix and sodium alginate) were added to the powders to prepare cylindrical pellets (diameter 10 mm) using a hydraulic press, and sintered in air at 1,700 °C for 6 h.

Inductively Coupled Plasma Atomic Emission Spectrophotometry was performed at the CNRS of Vernaison on the pellets to check the composition.

The reactivity with hydrogen was studied at 600 °C (expected operating temperature of a PCFC). Different 3-h treatments were run in a closed oven: in dry hydrogen, in moisturized hydrogen and in moisturized deuterium.

After each treatment, a proton diffusion profile was recorded by Secondary Ion Mass Spectroscopy (SIMS). These analyses were performed using a MIQ 256 Cameca Riber apparatus located in a ultra-high vacuum chamber (10^{-7} Pa). The content of $^1H^+$ ions versus depth was obtained using a Ar^+ primary ion source: 10 keV, incident angle of 45°, current of 5 or 50 nA.

3 Results and discussion

3.1 Structural, morphologic and chemical analysis

The homogeneity of the mixture of the four precursors was checked by XRD. Different samplings were performed in the batch: all the diffractograms were similar.

A slow heating ramp (100 °C h^{-1}) was used for the calcinations to decompose carbonates. The synthesized powders are single phased, with a cubic structure (Fig. 2). The results for the lattice parameter (refined with Celref software) and theoretical density are summarized in Table 1.

The density of the sintered pellets is about 90% (closed porosity). The use of these materials as electrolyte in PCFC required at least 95% relative density. However it has been shown [21] that porous samples exhibit a similar dependence of conductivity on water vapour pressure and temperature as do dense samples. So, the incorporation of water in samples with a density lower than 95% will give the same basic information as does the measurement on dense bodies.

Table 2 ICP-AES results: ICP stands for the experimental results, and TH for the theoretical values

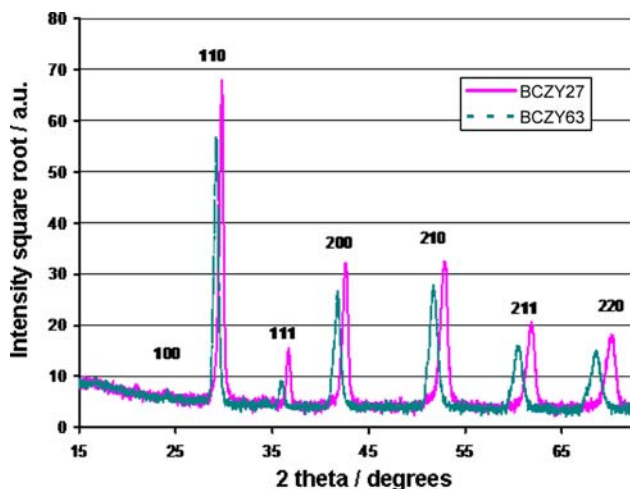|	Ba/Ce ICP	Ba/Zr ICP	Ba/Y ICP	Ba/Ce TH	Ba/Zr TH	Ba/Y TH
BCZY27	4.93 ± 0.2	2.24 ± 0.09	15.56 ± 0.6	4.92	2.15	15.44
BCZY63	1.66 ± 0.06	5.11 ± 0.2	15.15 ± 0.6	1.63	5.02	15.44

Fig. 3 XRD patterns for BCZY27 and BCZY63 pellets, sintered at 1,700 °C

The ICP-AES results (Table 2) reveal no evaporation of barium after heating at 1,700 °C for 6 h.

Polishing of the sintered samples is necessary to remove the defects from the surface. The XRD patterns of the pellets are shown in Fig. 3. Parasite phases such as ceria or zirconia, which appear when barium evaporates, are not present.

The grain size of the powders is between 200 and 500 nm (Fig. 4). The solid solution of cerate and zirconate exhibit a significant heat-resistant property which inhibits grain growth. Sintering is easier for cerates than for zirconates: Grain size is about 500 nm–1 μm for BCZY27 and 1–2 μm for BCZY63.

3.2 SIMS experiments

The analysed depth was between 1 and 3 μm. A depth profile was achieved on the pellet before treatment. The $^{138}Ba^+$ signal is used as a reference: it provides an

Fig. 4 SEM picture of BCZY27 powder (**a**), BCZY63 powder (**b**), BCZY27 pellet (**c**) and BCZY63 pellet (**d**)
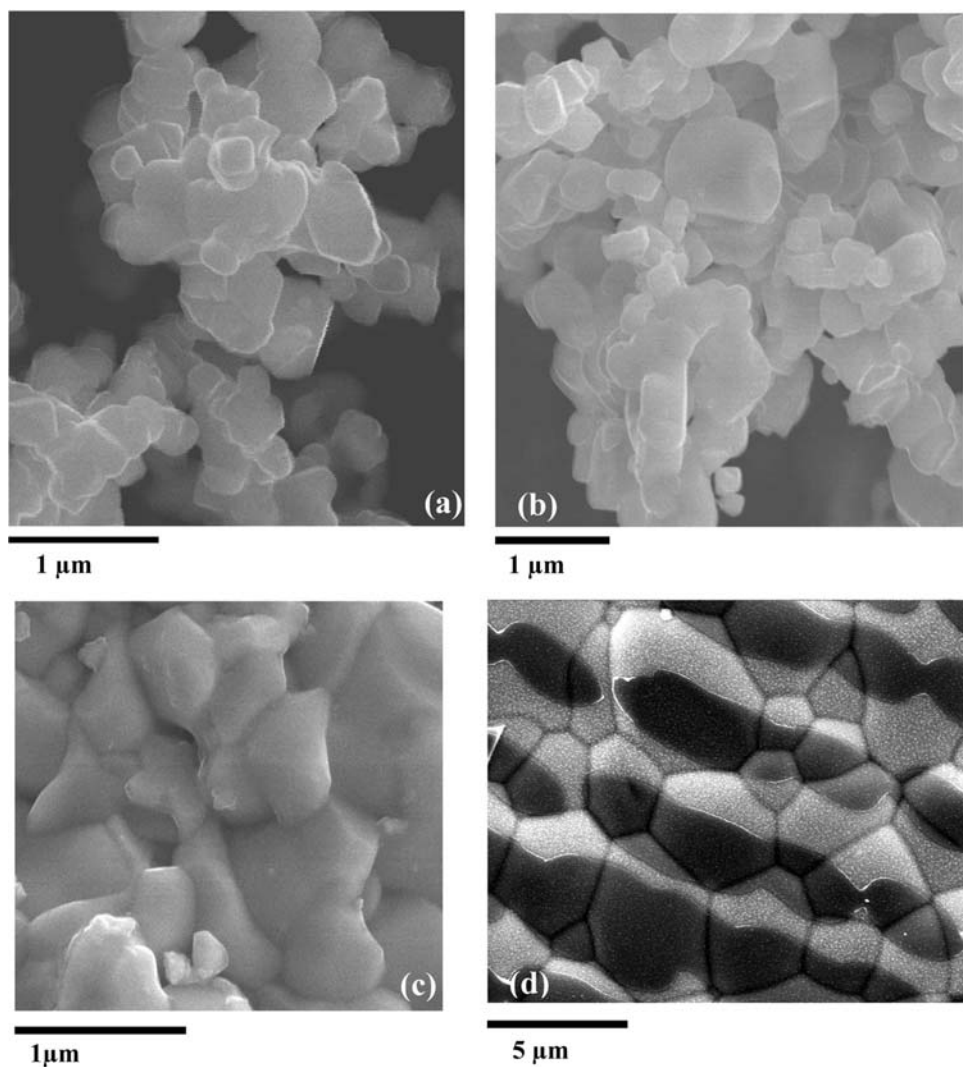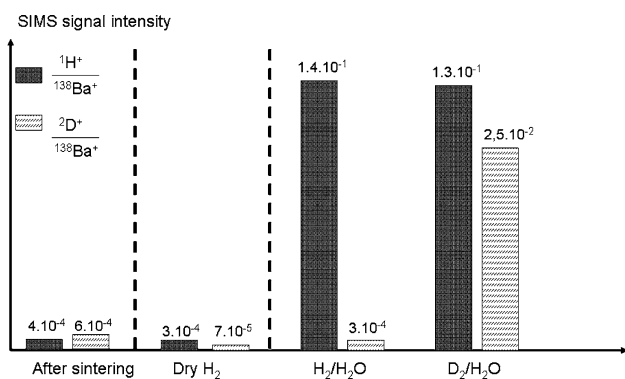
Fig. 5 Ratio of the intensity of the hydrogen (or deuterium) signal divided by the intensity of the barium signal, for different reducing atmospheres

Fig. 6 SIMS profiles in dry and wet hydrogen for BCZY27 and BCZY63, in wet deuterium and wet hydrogen for BCZY27

estimation of the expected value for an element present in the oxide. The $^1H^+$ signal (about 7,000 counts) is higher than the background (generally 100 counts). Protons are present in the sintered pellet. Indeed, conventional sintering was conducted in air. Water vapour was present while cooling and caused proton fixation in the sample. The ratio of the intensity of the hydrogen signal divided by the intensity of the barium signal (called R in the following paragraph) is about 4×10^{-4}. Figure 5 represents the dependence of R on the treatment.

The depth profiles obtained for the BCZY27 and BCZY63 pellets in dry hydrogen are similar and are presented in Fig. 6a, as well as those obtained in wet hydrogen. Only one signal for barium is plotted: there is no difference between the intensity of the barium signal for the pellet before and after treatment because of the logarithmic scale used for the intensity axis.

For the treatment in dry hydrogen, R is equal to 5×10^{-4} for BCZY27 and BCZY63. This value is similar to the one before treatment. So treatment at 600 °C for 3 h in dry hydrogen leads to no significant proton incorporation.

Incorporation of protons in the pellets is obvious when water is introduced (Fig. 6a). Indeed, protons are present on the SIMS profiles, for both the compositions and R increases to 1.3×10^{-1}.

Deuterium was used instead of hydrogen for isotopic exchange (Fig. 6b). The comparison between the H_2/H_2O and the D_2/H_2O profiles leads to the following remarks:

– The $^1H^+$ signal is similar ($R = 1.4 \times 10^{-1}$ for H_2/H_2O and $R = 1.3 \times 10^{-1}$ for D_2/H_2O) indicating that protons come from the dissociation of water vapour.
– The $^2D^+$ signal increases when deuterium is used instead of hydrogen. In this case, the presence of deuterium incorporated in the sample can be explained by isotopic exchanges (formation of D_2O).
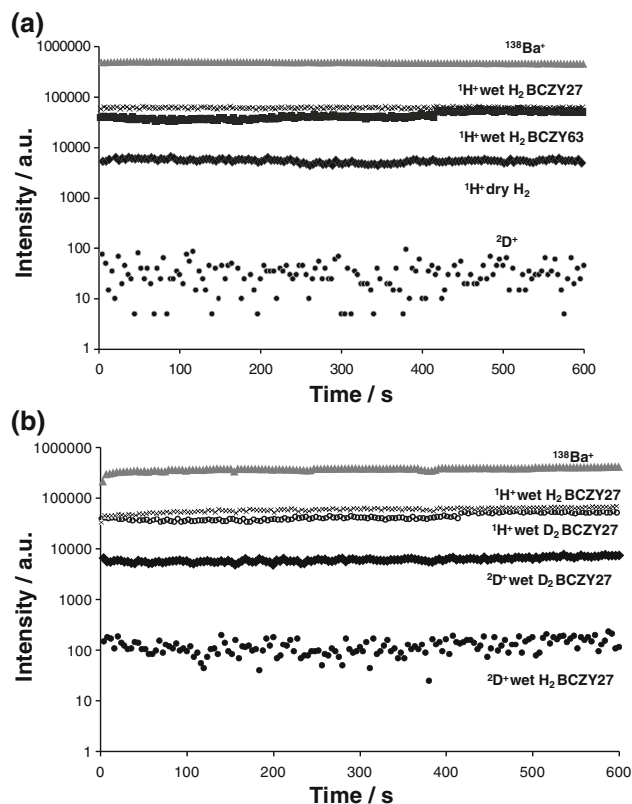
4 Conclusions

Very high temperatures are necessary to synthesize and sinter the BCZY compounds (1,400 °C for synthesis and 1,700 °C for sintering). The resulting pellets are not dense enough to be used in a cell, but the reactivity in reducing atmosphere can be studied.

Protons are not introduced significantly in the sample after treatment at 600 °C for 3 h in dry hydrogen. It is necessary to work in the cell configuration (with electrodes to collect electrons) to incorporate protons using hydrogen.

When water vapour is added to hydrogen (10% of the mix), the $^1H^+$ signal increases. The dissociation of water vapour does not create electrons, so this reaction takes place even with the sample without electrode. Isotope exchange is achieved and shows that protons come from water. Indeed, the $^1H^+$ signal had the same intensity for both treatments: H_2/H_2O and D_2/H_2O. D_2O is formed in the wet deuterium atmosphere, because of the isotopic exchange between D and H at 600 °C. D_2O dissociates at the sample surface, so deuterium is incorporated in the sample.

Finally, one should note the high diffusion of protons, as shown by the flatness of the proton depth profiles.

References

1. Schober T, Krug F, Schilling W (1997) Solid State Ion 97:369
2. Künstler K, Lang HJ, Maiwald A, Tomandl G (1998) Solid State Ion 107:221
3. Münch W, Kreuer KD, Seifert G, Maier J (2000) Solid State Ion 136–137:183
4. Bonanos N (2001) Solid State Ion 145:265
5. Scholten MJ, Schoonman J, Van Miltenburg JC, Oonk HAJ (1993) Solid State Ion 61:83
6. Taniguchi N, Nishimura C, Kato J (2001) Solid State Ion 145:349
7. Gopalan S, Virkar AV (1996) J Electrochem Soc 143:1386
8. Ryu KH, Haile SM (1999) Solid State Ion 125:355
9. Kreuer KD (1999) Solid State Ion 12:285
10. Bonanos N, Knight KS, Ellis B (1995) Solid State Ion 79:161
11. Scholten MJ, Schoonman J, Van Miltenburg JC (1999) Thermochim Acta 268:161
12. Shimada T, Wen C, Taniguchi N, Otomo J, Takahaschi H (2004) J Power Source 131:289
13. Katahira K, Kohchi Y, Shimura T, Iwahara H (2000) Solid State Ion 138:91
14. Kosacki I, Tuller HL (1995) Solid State Ion 80:223
15. Iwahara H (1996) Solid State Ion 9:86–88
16. Colomban P (1999) Ann Chim Sci Mat 24:1
17. Nowick AS, Du Y (1995) Solid State Ion 77:137
18. Norby T (1999) Solid State Ion 125:1
19. Hempelmann R (1996) Phys B 226:72
20. Agmon N (1995) Chem Phys Lett 224:456
21. Wang W, Virkar AV (2005) J Power Source 142:1